Submitted to ApJ Letters on 3 December, 2013.
Preprint typeset using LaTeX style emulateapj v. 11/10/09

THE MASS-RADIUS RELATION BETWEEN 63 EXOPLANETS SMALLER THAN 4 EARTH RADII

Lauren M. Weiss[1,†] & Geoffrey W. Marcy[1]
[1]B-20 Hearst Field Annex, Astronomy Department, University of California, Berkeley, CA 94720
Submitted to ApJ Letters on 3 December, 2013.

ABSTRACT

We study the masses and radii of 63 exoplanets smaller than $4R_\oplus$ with orbital periods shorter than 100 days. We find a nearly linear mass-radius relation: $M_\mathrm{P}/M_\oplus = 3.24\,(R_\mathrm{P}/R_\oplus)^{0.80}$, which is a shallower power-law index than in many previous mass-radius relations. The RMS of planet masses to this fit is 3.9 $M_\oplus$, and our best fit has reduced $\chi^2 = 3.5$, indicating a diversity in planet compositions below $4R_\oplus$. The mass-radius relation reflects that planet density decreases as radius increases, indicating that larger exoplanets have a significant fraction of volatiles by volume (such as H/He envelopes). Exoplanets have densities comparable to that of Earth at $R_\mathrm{P} \sim 1.5R_\oplus$, indicating likely rocky compositions among planets smaller than 1.5 $R_\oplus$. The scaling of the mass-radius relationship for exoplanets with $R_\mathrm{P} < 1.5R_\oplus$ is not well-constrained but if we include the solar system terrestrial planets, we find that a relationship of $M_\mathrm{P}/M_\oplus = 1.08\,(R_\mathrm{P}/R_\oplus)^{3.45}$ is a significant improvement over the nearly linear relationship. Analyzing just the exoplanets with $1.5 \leq R_\mathrm{P}/R_\oplus < 4$, we find that they are well described by a nearly flat relation: $M_\mathrm{P}/M_\oplus = 5.6 + 0.71R_\mathrm{P}/R_\oplus$ with reduced $\chi^2 = 3.5$, indicating that differences in masses in this size range are due to compositional variety.

1. INTRODUCTION

The Kepler Mission has found an abundance of planets with radii $R_\mathrm{P} < 4R_\oplus$ (Batalha et al. 2013). Although there are no planets between the size of Earth and Neptune in the solar system, occurrence calculations that debias the orbital geometry and completeness of the Kepler survey find that planets between the size of Earth and Neptune are common in our galaxy, occurring with orbital periods between 5 and 50 days around 24% of stars (Petigura et al. 2013). However, in many systems, it is difficult to measure the masses of such small planets because the gravitational acceleration these planets induce on their host stars or neighboring planets is challenging to detect with current telescopes and instruments. Obtaining measurements of the masses of these planets and characterizing their compositions is vital to understanding the formation and evolution of these planets.

Many authors have explored the relation between planet mass and radius as a means for understanding exoplanet compositions and as a predictive tool. Seager et al. (2007) predict the mass-radius relationship for planets of various compositions. The mass-radius relation in Lissauer et al. (2011), which is commonly used in literature to translate between planet masses and radii, is based on fitting a power law relation to Earth and Saturn only. Other works, such as Enoch et al. (2012); Kane & Gelino (2012); Weiss et al. (2013), determine empirical relations between mass and radius based on the exoplanet population.

Recent mass determinations of small planets motivate a new empirical mass-radius relation. Restricting the empirical mass-radius relation to small exoplanets will improve the goodness of fit, allowing better mass predictions and enabling a superior physical understanding of the processes that drive the mass-radius relation for small planets.

One challenge in determining a mass-radius relation for small planets is the large scatter in planet mass. At $2R_\oplus$, planets are observed to span a decade in density, from less dense than water to densities suggesting a solid iron composition. This scatter could result from measurement uncertainty or from compositional variety among low-mass exoplanets.

In this paper, we investigate mass-radius relationships for planets smaller than 4 Earth radii and explore a tentative mass-radius relationship for likely rocky planets smaller than 1.5 $R_\oplus$. We also investigate the extent to which system properties contribute to the scatter in the mass-radius relation by examining how these properties correlate with the residuals of the mass-radius relation.

2. SELECTING EXOPLANETS WITH MEASURED MASS AND RADIUS

We include all 19 planets smaller than $4R_\oplus$ with masses vetted on exoplanets.org, as of October 22, 2013. Twelve of these masses are determined by radial velocities (RVs), but the masses of the four Kepler-11 planets, Kepler-30 b, the two Kepler-36 planets, and the three KOI-152 (Kepler-79) planets are determined by transit timing variations (TTVs) (Lissauer et al. 2013; Sanchis-Ojeda et al. 2012; Carter et al. 2012; Jontof-Hutter et al. 2013). We include all 40 transiting planets with RV follow-up in Marcy et al. (2013) that are smaller than $4R_\oplus$, and one planet (KOI-94 b, R=1.7 $R_\oplus$) from Weiss et al. (2013). 55 Cnc e, Corot-7 b, and GJ 1214 b have been studied extensively, and we had to choose from the masses and radii reported in various studies. For 55 Cnc e, we use $M_\mathrm{P} = 8.38 \pm 0.39$, $R_\mathrm{P} = 1.990 \pm 0.084$ (Endl et al. 2012; Dragomir et al. 2013b); for Corot-7 b, we use $M_\mathrm{P} = 7.42 \pm 1.21$, $R_\mathrm{P} = 1.58 \pm 0.1$ (Hatzes et al. 2011), and for GJ 1214 b, we use $M_\mathrm{P} = 6.45 \pm 0.91$, $R_\mathrm{P} = 2.65 \pm 0.09$ (Carter et al. 2011). Histograms of the distributions of planet radius, mass, and density are shown in Figure 1, and the individual measurements of

† Supported by the NSF Graduate Student Fellowship, Grant DGE 1106400.

planet mass and radius are listed in Table 1.

The only selection criterion was that the exoplanets have $R_{\rm P} < 4R_\oplus$ and either a mass determination, a marginal mass determination, or a mass upper limit. There were no limits on stellar type, orbital period, or other system properties. The exoplanets all have $P < 100$ days. This is because the transit probability is very low for planets at long orbital periods and because short-period planets are often favored for RV and TTV studies.

2.1. *Inclusion of Mass Non-Detections*

For small exoplanets, uncertainties in the mass measurements can be of order the planet mass. Although one might advocate for only studying planets with well-determined ($> 3\sigma$) masses, imposing a significance criterion will bias the sample toward more massive planets at a given radius. This bias is especially pernicious for small planets, for which the planet-induced RV signal can be small ($\sim 1 {\rm m\,s^{-1}}$) compared to the noise from stellar activity ($\sim 2 {\rm m\,s^{-1}}$) and Poisson photon noise ($\sim 2 {\rm m\,s^{-1}}$). We must include the marginal mass detections and non-detections in order to minimize bias in planet masses at a given radius.

Marcy et al. (2013) fix the orbital period and orbital phase of the planets at the transit ephemeris, allowing only the RV semi-amplitude induced by the planets to vary. Neither the stellar activity nor the Poisson photon noise is expected to phase with the orbit of a small planet. However, random fluctuations due to the stellar activity and photon noise can produce RVs that are low when they should be high and high when they should be low, or vice versa. Random noise in the RVs that phases with the expected planet signal will result in an over-estimate of planet mass. To minimize this bias from noise, we must include the solutions that, due to random noise, are anti-phased with the expected planet signal. Marcy et al. (2013) allow a negative semi-amplitude in the Keplerian fit to the RVs and report the peak and 68^{th} percentiles of the posterior distribution of the semi-amplitude; the peak often corresponds to a "negative" planet mass. We include non-detections to avoid statistical bias toward large planet masses at a given radius.

Including literature values, which typically only report planet mass if the planet mass is detected with high confidence, slightly biases our sample toward higher masses at a given radius. We include the literature values to provide a larger sample of exoplanets.

3. THE MASS-RADIUS RELATION FOR 63 SMALL EXOPLANETS

The mass-radius plot for planets smaller than 4 $R_\oplus$ shown in Figure 2 (left) shows that, on average, exoplanet mass increases with increasing radius, indicating an underlying correlation in the individual exoplanet masses and radii. We calculate the probability that mass and radius are uncorrelated for planets smaller than $4R_\oplus$ by calculating the Pearson R correlation coefficient: $r = 0.61$. In our sample of 63 exoplanets, the probability that these data are uncorrelated given $r = 0.61$ is 2×10^{-7}. Thus, the masses and radii of planets between the sizes of Earth and Neptune are correlated.

Figure 2 shows the mass vs. radius and density vs. radius of 63 exoplanets examined here (although some outliers are excluded). To guide the eye, we show the weighted mean exoplanet mass and density in bins of width 0.5 $R_\oplus$. The weighted mean mass and density were not used in calculating the fits.

To illustrate how this population of exoplanets compares to our solar system, we indicate the solar system planets in Figure 2. A quadratic fit to the exoplanet population happens to line up with the solar system planets (Lissauer et al. 2011), but has a reduced χ^2 that is twice as large as the linear fit to the exoplanets. Since most of the exoplanets in this sample have $P < 50$ days, we do not expect them to behave the same way as Uranus and Neptune, which have orbital periods of tens of thousands of days.

We present several empirical relations between planet mass and radius, and between density and radius, which are illustrated in Figure 2. The right panel in Figure 2 shows that planets achieve an Earth-density at about 1.5 $R_\oplus$. Rocky planets smaller than $1.5R_\oplus$ might be better described with a different functional form. We consider independent relations for planets satisfying $R_{\rm P} < 1.5R_\oplus$ to determine if relations consistent with rocky compositions better describe those planets.

3.1. *The Mass-Radius Relation for $R_{\rm P} < 4R_\oplus$*

3.1.1. *A Power-Law Mass-Radius Relation*

The power-law fit to the masses and radii for $R_{\rm P} < 4R_\oplus$ yields:

$$\frac{M_{\rm P}}{M_\oplus} = 3.24 \left(\frac{R_{\rm P}}{R_\oplus} \right)^{0.80} \quad (1)$$

with reduced $\chi^2 = 3.5$ and RMS=3.9 $M_\oplus$. A parametric bootstrap error analysis of 1000 trials gives these uncertainties in the coefficients: $c_0 = 3.24 \pm 0.47$, $c_1 = 0.80 \pm 0.11$.

3.1.2. *A Linear Mass-Radius Relation*

The weighted linear fit to the data for $R_{\rm P} < 4R_\oplus$ yields:

$$M_{\rm P}/M_\oplus = 0.81 + 2.36\ R_{\rm P}/R_\oplus \quad (2)$$

with reduced $\chi^2 = 3.6$ and RMS= $3.9M_\oplus$. The standard errors for the weighted linear fit are *slope* $= 2.36 \pm 0.59$, *intercept* $= 0.81 \pm 1.25$. We allow the intercept to float to accommodate the possibility of a different mass-radius relation for small bodies. As evidenced by their comparable χ^2 and RMS, the power law solution and the weighted linear fit describe the masses and radii equally well with equally few parameters, and therefore either is an appropriate description of the data. Both represent a nearly linear relation between planet mass and radius for planets smaller than 4 $R_\oplus$.

3.2. *A Break in the Mass-Radius Relation at 1.5 $R_\oplus$*

To investigate the possibility of a different relationship between the masses and radii of the likely rocky exoplanets, for which we expect little to no volatile envelope and low bulk compressibility, we do an independent analysis for planets smaller than 1.5 $R_\oplus$. We choose $1.5R_\oplus$ because this is where the weighted mean exoplanet density crosses the Earth-composition density curve from Seager et al. (2007, see Figure 2). Exoplanets smaller than 1.5 $R_\oplus$mostly have mass uncertainties of order the planet

Table 1
Exoplanets with Masses or Mass Upper Limits and $R_{\rm P} < 4R_\oplus$

Name	Per (d)	Mass ($M_\oplus$)	Radius ($R_\oplus$)	Flux[a] ($F_\oplus$)	First Ref.	Mass, Radius Ref.
[b]55 Cnc e	0.737	8.38±0.39	1.990±0.084	2439.690	McArthur et al. (2004)	Endl et al. (2012), Dragomir et al. (2013a)
CoRoT-7 b	0.854	7.42±1.21	1.58±0.1	1779.433	Queloz et al. (2009), Léger et al. (2009)	Hatzes et al. (2011)
GJ 1214 b	1.580	6.45±0.91	2.65±0.09	16.631	Charbonneau et al. (2009)	Carter et al. (2011)
HD 97658 b	9.491	7.87±0.73	2.34±0.16	48.106	Howard et al. (2011)	Dragomir et al. (2013b)
Kepler-10 b	0.837	4.60±1.26	1.46±0.02	3675	Batalha et al. (2011)	Batalha et al. (2011)
[c]Kepler-11 b	10.304	1.90±1.20	1.80±0.04	126.512	Lissauer et al. (2011)	Lissauer et al. (2013)
[c]Kepler-11 c	13.024	2.90±2.20	2.87±0.06	91.443	Lissauer et al. (2011)	Lissauer et al. (2013)
[c]Kepler-11 d	22.684	7.30±1.10	3.12±0.07	43.563	Lissauer et al. (2011)	Lissauer et al. (2013)
[c]Kepler-11 f	46.689	2.00±0.80	2.49±0.06	16.747	Lissauer et al. (2011)	Lissauer et al. (2013)
Kepler-18 b	3.505	6.90±3.48	2.00±0.10	462.244	Borucki et al. (2011)	Cochran et al. (2011)
Kepler-20 b	3.696	8.47±2.12	1.91±0.16	346.711	Borucki et al. (2011)	Gautier et al. (2012)
Kepler-20 c	10.854	15.73±3.31	3.07±0.25	82.445	Borucki et al. (2011)	Gautier et al. (2012)
Kepler-20 d	77.612	7.53±7.22	2.75±0.23	5.985	Borucki et al. (2011)	Gautier et al. (2012)
[c]Kepler-30 b	29.334	11.3±1.4	3.90 ±0.20	21.496	Borucki et al. (2011)	Sanchis-Ojeda et al. (2012)
[c]Kepler-36 b	13.840	4.46±0.30	1.48±0.03	217.365	Borucki et al. (2011)	Carter et al. (2012)
[c]Kepler-36 c	16.239	8.10±0.53	3.68±0.05	175.646	Carter et al. (2012)	Carter et al. (2012)
Kepler-68 b	5.399	8.30±2.30	2.31±0.03	409.092	Borucki et al. (2011)	Gilliland et al. (2013)
Kepler-68 c	9.605	4.38±2.80	0.95±0.04	189.764	Batalha et al. (2013)	Gilliland et al. (2013)
Kepler-78 b	0.354	1.69±0.41	1.20±0.09	3093.388	Sanchis-Ojeda et al. (2013)	Howard et al. (2013)
Kepler-100 c	12.816	0.85±4.00	2.20±0.05	213.371	Borucki et al. (2011)	Marcy et al. (2013)
Kepler-100 b	6.887	7.34±3.20	1.32±0.04	472.831	Borucki et al. (2011)	Marcy et al. (2013)
Kepler-100 d	35.333	-4.36±4.10	1.61±0.05	55.812	Borucki et al. (2011)	Marcy et al. (2013)
Kepler-93 b	4.727	2.59±2.00	1.50±0.03	220.120	Borucki et al. (2011)	Marcy et al. (2013)
Kepler-102 e	16.146	8.93±2.00	2.22±0.07	17.278	Borucki et al. (2011)	Marcy et al. (2013)
Kepler-102 d	10.312	3.80±1.80	1.18±0.04	31.184	Borucki et al. (2011)	Marcy et al. (2013)
Kepler-102 f	27.454	0.62±3.30	0.88±0.03	8.250	Borucki et al. (2011)	Marcy et al. (2013)
Kepler-102 c	7.071	-1.58±2.00	0.58±0.02	51.315	Borucki et al. (2011)	Marcy et al. (2013)
Kepler-102 b	5.287	0.41±1.60	0.47±0.02	78.407	Borucki et al. (2011)	Marcy et al. (2013)
KOI-94 b	3.743	10.50±4.60	1.71±0.16	1155.374	Batalha et al. (2013)	Weiss et al. (2013)
Kepler-94 b	2.508	10.84±1.40	3.51±0.15	214.674	Borucki et al. (2011)	Marcy et al. (2013)
Kepler-103 b	15.965	14.11±4.70	3.37±0.09	124.197	Borucki et al. (2011)	Marcy et al. (2013)
Kepler-106 c	13.571	10.44±3.20	2.50±0.32	84.462	Borucki et al. (2011)	Marcy et al. (2013)
Kepler-106 e	43.844	11.17±5.80	2.56±0.33	15.645	Borucki et al. (2011)	Marcy et al. (2013)
Kepler-106 b	6.165	0.15±2.80	0.82±0.11	239.077	Borucki et al. (2011)	Marcy et al. (2013)
Kepler-106 d	23.980	-6.39±7.00	0.95±0.13	43.146	Borucki et al. (2011)	Marcy et al. (2013)
Kepler-95 b	11.523	13.00±2.90	3.42±0.09	182.708	Borucki et al. (2011)	Marcy et al. (2013)
Kepler-109 b	6.482	1.30±5.40	2.37±0.07	444.879	Borucki et al. (2011)	Marcy et al. (2013)
Kepler-109 c	21.223	2.22±7.80	2.52±0.07	94.934	Borucki et al. (2011)	Marcy et al. (2013)
Kepler-48 b	4.778	3.94±2.10	1.88±0.10	168.932	Borucki et al. (2011)	Marcy et al. (2013)
Kepler-48 c	9.674	14.61±2.30	2.71±0.14	225.109	Borucki et al. (2011)	Marcy et al. (2013)
Kepler-48 d	42.896	7.93±4.60	2.04±0.11	13.545	Borucki et al. (2011)	Marcy et al. (2013)
Kepler-79 b	13.4845	10.9±6.70	3.47±0.07	161.456472	Borucki et al. (2011)	Jontof-Hutter et al. (2013)
Kepler-79 c	27.4029	5.9±2.10	3.72±0.08	63.225260	Borucki et al. (2011)	Jontof-Hutter et al. (2013)
Kepler-79 e	81.0659	4.1±1.15	3.49±0.14	14.833204	Borucki et al. (2011)	Jontof-Hutter et al. (2013)
Kepler-113 c	8.925	-4.60±6.20	2.19±0.06	50.981	Borucki et al. (2011)	Marcy et al. (2013)
Kepler-113 b	4.754	7.10±3.30	1.82±0.05	63.986	Borucki et al. (2011)	Marcy et al. (2013)
Kepler-25 b	6.239	9.60±4.20	2.71±0.05	667.269	Borucki et al. (2011)	Marcy et al. (2013)
Kepler-37 d	39.792	1.87±9.08	1.94±0.06	7.710	Borucki et al. (2011)	Marcy et al. (2013)
Kepler-37 c	21.302	3.35±4.00	0.75±0.03	16.291	Borucki et al. (2011)	Marcy et al. (2013)
Kepler-37 b	13.367	2.78±3.70	0.32±0.02	37.373	Borucki et al. (2011)	Marcy et al. (2013)
Kepler-68 b	5.399	5.97±1.70	2.33±0.02	375.530	Borucki et al. (2011)	Marcy et al. (2013)
Kepler-68 c	9.605	2.18±3.50	1.00±0.02	220.199	Borucki et al. (2011)	Marcy et al. (2013)
Kepler-96 b	16.238	8.46±3.40	2.67±0.22	73.950	Borucki et al. (2011)	Marcy et al. (2013)
Kepler-131 b	16.092	16.13±3.50	2.41±0.20	71.656	Borucki et al. (2011)	Marcy et al. (2013)
Kepler-131 c	25.517	8.25±5.90	0.84±0.07	28.891	Borucki et al. (2011)	Marcy et al. (2013)
Kepler-97 b	2.587	3.51±1.90	1.48±0.13	851.551	Borucki et al. (2011)	Marcy et al. (2013)
Kepler-98 b	1.542	3.55±1.60	1.99±0.22	1581.816	Borucki et al. (2011)	Marcy et al. (2013)
Kepler-99 b	4.604	6.15±1.30	1.48±0.08	90.372	Borucki et al. (2011)	Marcy et al. (2013)
Kepler-406 b	2.426	6.35±1.40	1.43±0.03	713.204	Borucki et al. (2011)	Marcy et al. (2013)
Kepler-406 c	4.623	2.71±1.80	0.85±0.03	291.503	Borucki et al. (2011)	Marcy et al. (2013)
Kepler-407 b	0.669	0.06±1.20	1.07±0.02	3645.770	Borucki et al. (2011)	Marcy et al. (2013)
KOI-1612.01	2.465	0.48±3.20	0.82±0.03	1691.964	Borucki et al. (2011)	Marcy et al. (2013)
Kepler-409 b	68.958	2.69±6.20	1.19±0.03	6.165	Borucki et al. (2011)	Marcy et al. (2013)

[a] Incident stellar flux is calculated as $F/F_\oplus = (R_\star/R_\odot)^2 (T_{\rm eff}/5778{\rm K})^4 a^{-2} \sqrt{1/(1-e)^2}$, where a is the semi-major axis in A.U. and e is the eccentricity.

[b] Mass is from Endl et al. (2012), radius is from Dragomir et al. (2013a). The density is calculated from these values.

[c] Planet mass determined by TTVs of a neighboring planet

mass, except for CoRoT-7 b, Kepler-10 b, and Kepler-78 b. Therefore, this mass-radius relation is poorly determined. The best power-law fit to exoplanets smaller that 1.5 $R_\oplus$gives:

$$\frac{M_\mathrm{P}}{M_\oplus} = 0.94 \left(\frac{R_\mathrm{P}}{R_\oplus} \right)^{4.02} \quad (3)$$

with reduced $\chi^2 = 0.88$ and RMS= $3.0 M_\oplus$. For comparison, we apply the power law fit in equation 1 to the likely rocky planets, obtaining reduced $\chi^2 = 1.8$ and RMS= $2.9 M_\oplus$. We cannot empirically distinguish between these two fits to the likely rocky exoplanets. However, for rocky planets that are slightly compressible, we expect $M_\mathrm{P} \propto R_\mathrm{P}^{3+\alpha}$, where $\alpha > 0$. Therefore, we prefer equation 3 to equation 1 for $R_\mathrm{P} < 1.5 R_\oplus$.

Because the equation of state for rocky planets should not depend on the orbital period of the planet or incident flux on the planet, we can include the terrestrial solar system planets (Mercury, Venus, Earth, Mars) in a power law fit to the terrestrial planets. We impose uncertainties of 10% in their masses and 5% in their radii so that the solar system planets will contribute to, but not dominate, the fit to the terrestrial planets. The best power-law fit for exoplanets and solar system planets with $R_\mathrm{P} < 1.5 R_\oplus$ gives:

$$\frac{M_\mathrm{P}}{M_\oplus} = 1.08 \left(\frac{R_\mathrm{P}}{R_\oplus} \right)^{3.45} \quad (4)$$

with reduced $\chi^2 = 1.3$ and RMS = $2.7 M_\oplus$. A parametric bootstrap error analysis of 1000 trials gives these uncertainties in the coefficients: $c_0 = 1.08 \pm 1.09$, $c_1 = 3.45 \pm 8.44$. The large uncertainties in the masses and small number of planets allow a variety of fits to the masses and radii if the data are perturbed.

For planets satisfying $1.5 \leq R_\mathrm{P}/R_\oplus < 4$, we find:

$$\frac{M_\mathrm{P}}{M_\oplus} = 5.6 + 0.71 \frac{R_\mathrm{P}}{R_\oplus} \quad (5)$$

with reduced $\chi^2 = 3.5$ and RMS=4.7 $M_\oplus$.

The similarity between equations 3 and 5 demonstrates that the solar system planets are not significantly changing the result. However, the solar system planets disfavor the nearly linear power law fit in equation 1, as applied to planets smaller than $1.5 R_\oplus$. Including the solar system planets and their artificial errors raises the *reduced* χ^2 minimization to 3500, favoring the higher power law index of equation 5 over the shallower relation for the sub-Neptunes described in equation 1.

These empirical relations are summarized in Table 1.

4. DISCUSSION

4.1. *Interpretation of the Mass-Radius Relation*

The correlation between exoplanet mass and radius for $R_\mathrm{P} < 4 R_\oplus$ for close-in planets indicates that Earth-size planets are less massive than Neptune-size planets. The moderate reduced χ^2 values for the mass-radius relations ($\chi^2 \approx 3.5$) presented here indicate that measurement errors do not explain the variation in planet mass at a given radius. A diversity of planet compositions better explains the large scatter in planet mass.

Although most of the planets smaller than 1.5 $R_\oplus$ do not have mass detections better than 2σ, their ensemble provides weak constraints on the expected mass of planets smaller than Earth. None of the planets smaller than Earth has a mass larger than $10 M_\oplus$, and most have $M_\mathrm{P} < 5 M_\oplus$. CoRoT-7 b, Kepler-78 b and Kepler-10 b provide significant mass measurements in this range. However, these three exoplanets are not sufficient to constrain the power law relation that best fits exoplanets smaller than $1.5 R_\oplus$. The inclusion of solar system planets favors equation 5 for planets smaller than $1.5 R_\oplus$, but more discoveries of rocky exoplanets are necessary to hone this relation.

The Seager et al. (2007) density-radius relation for Earth composition predicts that density increases with planet radius due to the compression of solids, and equation 5 is consistent with this interpretation. However, for planets larger than 1.5 $R_\oplus$, density decreases with increasing planet radius due to an increasing fraction of volatiles. It is not clear where this transition occurs due to the large uncertainties in the data. Two possible interpretations are that the transition occurs at $1.5 R_\oplus$, where the weighted mean density rises above the density of an Earth-composition planet, or at $1.0 R_\oplus$, where the Earth-composition curve from Seager et al. (2007) crosses the polynomial density-radius relation that describes planets smaller than $4 R_\oplus$.

Lissauer et al. (2011), Enoch et al. (2012), Kane & Gelino (2012), and Weiss et al. (2013) suggest that the mass-radius relation is more like $M_\mathrm{P} \propto R_\mathrm{P}^2$ for small exoplanets. However, these studies include Saturn or Saturn-like planets at the high-mass end of their "small planet" populations. Such planets are better described as part of the giant planet population and are not useful in determining an empirical mass-radius relation of predictive power for small exoplanets. Excluding Saturn-like planets gives a near-linear mass-radius relation for small planets.

In a study of planets with $M_\mathrm{P} < 20 M_\oplus$, Wu & Lithwick (2013) find $M_\mathrm{P}/M_\oplus = 3 R_\mathrm{P}/R_\oplus$ in a sample of 22 pairs of planets that exhibit strong anti-correlated TTVs in the *Kepler* data. Our independent assessment of 63 exoplanets, 51 of which are not analyzed in Wu & Lithwick (2013), is consistent with this result. Wu & Lithwick (2013) note that a linear relation between planet mass and radius is dimensionally consistent with a constant escape velocity from the planet (i.e. $v_\mathrm{esc}^2 \sim M_\mathrm{P}/R_\mathrm{P}$). The linear mass-radius relation might result from photoevaporation of the atmospheres of small planets near their stars (Lopez et al. 2012).

4.2. *Masses from TTVs are Lower than Masses from RVs*

We have included planets with masses determined by the TTVs observed in a neighboring planet in Table 1, Figure 2, and the mass-radius relations in equations 1-5. The TTV masses included in this work are the result of dynamical modeling that reproduces the observed TTV signatures in the Kepler light curve. Planets with TTV-determined masses are marked with superscript c in Table 1. In Figure 2, the TTV planets are shown as orange points; they are systematically less massive than the RV-discovered planets of the same radii (also see Jontof-Hutter et al. (2013)). A T-test comparing the residual masses from the RVs to the TTVs for planets larger than 1.0 $R_\oplus$results in a two-tailed P-value of 0.06, indicating

Table 2
Empirical Mass-Radius and Density-Radius Relations

Planet Size	Equation	Reduced χ^2	RMS
$R_P < 4R_\oplus$	$\frac{M_P}{M_\oplus} = 3.24 \left(\frac{R_P}{R_\oplus}\right)^{0.80}$	3.5	3.9 $M_\oplus$
$R_P < 4R_\oplus$	$M_P/M_\oplus = 0.81 + 2.36\ R_P/R_\oplus$	3.6	3.9 $M_\oplus$
$1.5 \leq R_P/R_\oplus < 4$	$\frac{M_P}{M_\oplus} = 5.6 + 0.71\ \frac{R_P}{R_\oplus}$	3.5	4.7 $M_\oplus$
$R_P < 1.5R_\oplus$	$\frac{M_P}{M_\oplus} = 0.94 \left(\frac{R_P}{R_\oplus}\right)^{4.02}$	0.88	3.0 $M_\oplus$
[a] $R_P < 1.5R_\oplus$	$\frac{M_P}{M_\oplus} = 1.08 \left(\frac{R_P}{R_\oplus}\right)^{3.45}$	1.3	2.7 $M_\oplus$

[a] Including terrestrial solar system planets Mercury, Venus, Earth, and Mars.

the two samples, if drawn from the same distribution, would be this discrepant 9% of the time.

The systematic difference between the TTV and RV masses is unlikely to stem from a bias in the RVs. Either the TTVs are systematically underestimating planet masses (possibly because other planets in the system damp the TTVs), or compact systems amenable to detection through TTVs have lower-density planets than non-compact systems (e.g. the Kepler-11 system, Lissauer et al. 2013). That Wu & Lithwick (2013) also find $M_P/M_\oplus \approx 3\,(R_P/R_\oplus)$ suggests that the TTV masses might be reliably systematically lower.

4.3. *Absence of Strong Correlations to Residuals*

We investigate how the residual mass correlates with various orbital properties and physical properties of the star. We adopt equation 1, and the residual mass is the measured minus predicted planet mass at a given radius. The quantities we correlate against are: planet orbital period, planet semi-major axis, the incident flux from the star on the planet, stellar mass, stellar radius, stellar surface gravity, stellar metallicity, stellar age, and stellar velocity times the sine of the stellar spin axis inclination (which are obtained through exoplanets.org or the papers cited in Table 1). In these data, the residual mass does not sternly correlate with any of these properties.

We find possible evidence of a correlation between residual planet mass and stellar metallicity for planets smaller than $4R_\oplus$. The Pearson R-value of the correlation is 0.25, resulting in a probability of 7% that the residual planet mass and stellar metallicity are not correlated, given the residual masses and metallicites. However, given that we looked for correlations among 9 pairs of variables, the probability of finding a 93.6% confidence correlation in any of the 9 trials due to random fluctuation is $1 - 0.936^9 = 0.45$, meaning there is only a 55% chance that the apparent metallicity correlation is real.

5. CONCLUSIONS

For exoplanets with $R_P < 4R_\oplus$ and $P < 100$ days, planet mass increases with radius nearly linearly, indicating that larger planets have substantially more volatiles than smaller planets.

The mass-radius relation achieves the density of an Earth-composition planet at approximately 1.5 $R_\oplus$. Planets smaller than $1.5R_\oplus$ are typically denser than Earth-composition and likely rocky, whereas exoplanets larger than $1.5R_\oplus$ are usually less dense than Earth-composition and likely contain a substantial fraction (by volume) of volatiles.

We recommend the following mass-radius relations for predictive purposes:

$$M_P/M_\oplus = 3.24\,(R_P/R_\oplus)^{0.80} \qquad (R_P > 1.5R_\oplus),$$

$$M_P/M_\oplus = 1.08\,(R_P/R_\oplus)^{3.45} \qquad (R_P < 1.5R_\oplus).$$

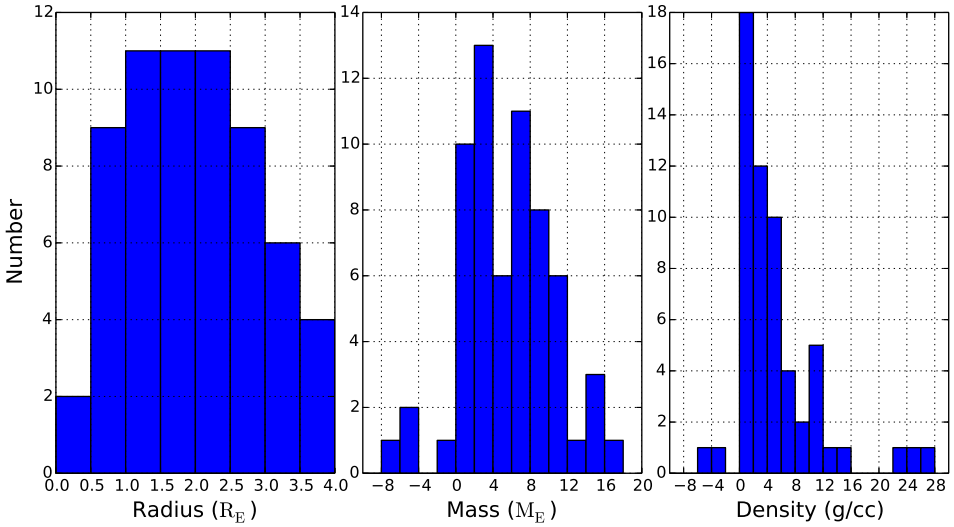

Figure 1. Histograms of exoplanet radii, masses, and densities for the 63 exoplanets smaller then 4 Earth radii with measured masses or mass upper-limits. Some mass and density outliers are excluded from these plots, but are included in Table 1 and the fits.

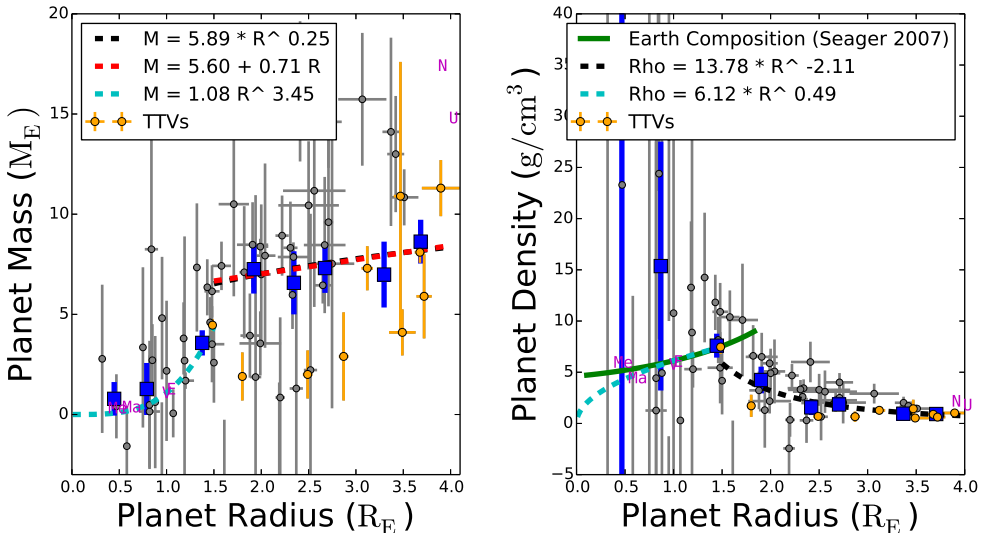

Figure 2. **Left:** Mass vs. radius for 63 exoplanets and 1σ error bars. Gray points have RV-determined masses; orange points have TTV-determined masses. The dashed lines are empirical fits mass-radius relations; see equations 1, 2, and 5. The blue points are the weighted mean exoplanet mass in bins of $0.5R_\oplus$, with error bars representing the uncertainty in the means. The weighted means were not used in calculating the fits. The magenta letters indicate solar system planets, which were used only in the cyan fit (equation 5). **Right:** Density vs. radius for 63 exoplanets and 1σ error bars. Note that no exoplanets smaller than $1R_\oplus$ have densities determined to better than 6.5 g cm^{-3}. The blue points are the weighted mean densities in bins of $0.5R_\oplus$. The Seager et al. (2007) density-radius solution for Earth's composition (32.5% Fe, 67.5% $MgSiO_3$) is the solid green line. The dashed line is the empirical fit between planet density and radius; see equation **??**. Planets larger than 1.5 $R_\oplus$are less dense than Earth composition, indicating that they probably contain a significant fraction of volatiles. Some mass and density outliers are excluded from these plots, but are included in the fits.

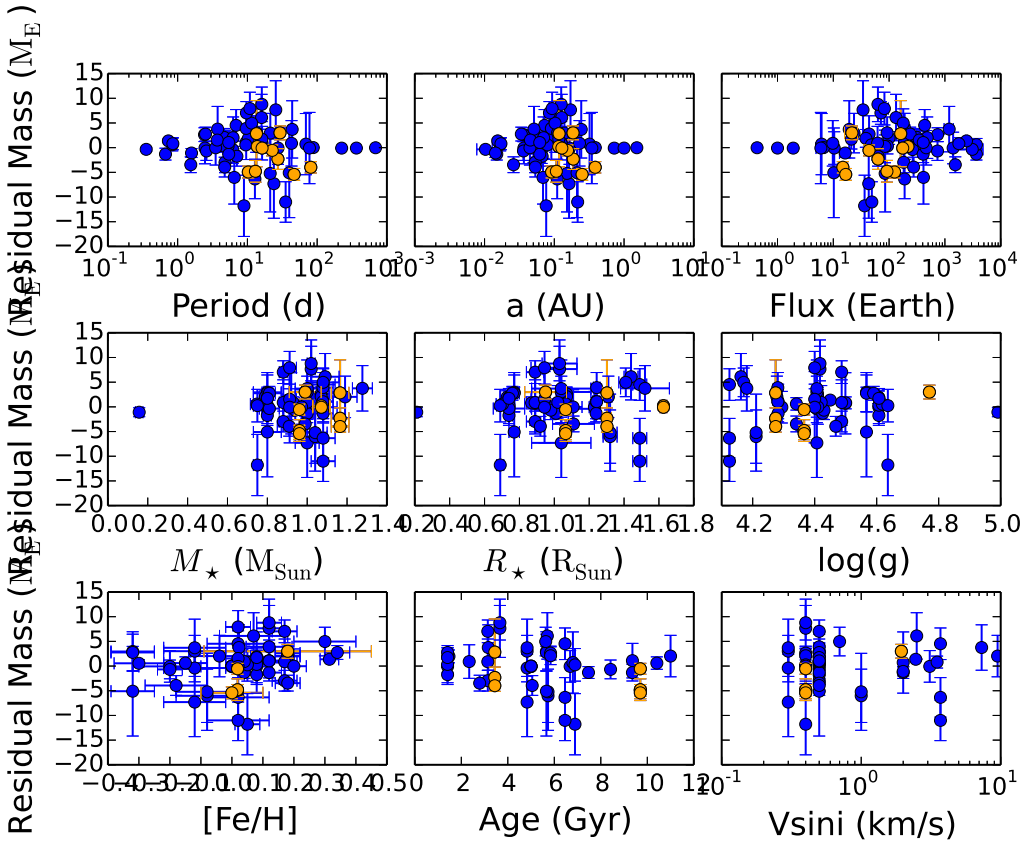

Figure 3. Mass residuals (measured minus the mass predicted from equation 1) versus (top left to bottom right): planet orbital period, planet semi-major axis, incident stellar flux, stellar mass, stellar radius, surface gravity, metallicity (compared to solar), stellar age, and stellar $v\sin i$. Error bars are 1σ uncertainties, and the orange points are residuals of the TTV-determined masses. None of the residuals show a significant correlation.

REFERENCES

Batalha, N. M., Borucki, W. J., Bryson, S. T., et al. 2011, ApJ, 729, 27
Batalha, N. M., Rowe, J. F., Bryson, S. T., et al. 2013, ApJS, 204, 24
Borucki, W. J., Koch, D. G., Basri, G., et al. 2011, ApJ, 736, 19
Carter, J. A., Winn, J. N., Holman, M. J., et al. 2011, ApJ, 730, 82
Carter, J. A., Agol, E., Chaplin, W. J., et al. 2012, Science, 337, 556
Charbonneau, D., Berta, Z. K., Irwin, J., et al. 2009, Nature, 462, 891
Cochran, W. D., Fabrycky, D. C., Torres, G., et al. 2011, ApJS, 197, 7
Dragomir, D., Matthews, J. M., Winn, J. N., Rowe, J. F., & MOST Science Team. 2013a, ArXiv e-prints
Dragomir, D., Matthews, J. M., Eastman, J. D., et al. 2013b, ApJ, 772, L2
Endl, M., Robertson, P., Cochran, W. D., et al. 2012, ApJ, 759, 19
Enoch, B., Collier Cameron, A., & Horne, K. 2012, A&A, 540, A99
Gautier, III, T. N., Charbonneau, D., Rowe, J. F., et al. 2012, ApJ, 749, 15
Gilliland, R. L., Marcy, G. W., Rowe, J. F., et al. 2013, ApJ, 766, 40
Hatzes, A. P., Fridlund, M., Nachmani, G., et al. 2011, ApJ, 743, 75
Howard, A. W., Johnson, J. A., Marcy, G. W., et al. 2011, The Astrophysical Journal, 726, 73
Howard, A. W., Sanchis-Ojeda, R., Marcy, G. W., et al. 2013, ArXiv e-prints
Jontof-Hutter, D., Lissauer, J. J., Rowe, J. F., & Fabrycky, D. C. 2013, ArXiv e-prints
Kane, S. R., & Gelino, D. M. 2012, PASP, 124, 323
Léger, A., Rouan, D., Schneider, J., et al. 2009, A&A, 506, 287
Lissauer, J. J., Fabrycky, D. C., Ford, E. B., et al. 2011, Nature, 470, 53
Lissauer, J. J., Jontof-Hutter, D., Rowe, J. F., et al. 2013, ApJ, 770, 131
Lopez, E. D., Fortney, J. J., & Miller, N. 2012, ApJ, 761, 59
Marcy, G. W., Isaacson, H., & Rowe, J. F. 2013, in prep.
McArthur, B. E., Endl, M., Cochran, W. D., et al. 2004, ApJ, 614, L81
Petigura, E. A., Marcy, G. W., & Howard, A. W. 2013, ApJ, 770, 69
Queloz, D., Bouchy, F., Moutou, C., et al. 2009, A&A, 506, 303
Sanchis-Ojeda, R., Rappaport, S., Winn, J. N., et al. 2013, ApJ, 774, 54
Sanchis-Ojeda, R., Fabrycky, D. C., Winn, J. N., et al. 2012, Nature, 487, 449
Seager, S., Kuchner, M., Hier-Majumder, C. A., & Militzer, B. 2007, ApJ, 669, 1279
Weiss, L. M., Marcy, G. W., Rowe, J. F., et al. 2013, ApJ, 768, 14
Wu, Y., & Lithwick, Y. 2013, ApJ, 772, 74